New type of centrifugal instability in a thin rotating spherical layer

IOP Conf. Series: Journal of Physics: Conf. Series 1163 (2019) 012011 doi:10.1088/1742-6596/1163/1/012011

New type of centrifugal instability in a thin rotating spherical layer

D Zhilenko[1], O Krivonosova[1] and M Gritsevich[2,3]

[1] Moscow State University, GSP-1, Leninskie Gory, 119991,Moscow, Russia
[2] Department of Physics, University of Helsinki, Gustaf Hällströmin katu 2a, FI-00014 Helsinki, Finland
[3] Institute of Physics and Technology, Ural Federal University,Mira str. 19, 620002, Ekaterinburg, Russia

E-mail: jilenko@imec.msu.ru

Abstract. We numerically model the instability of viscous incompressible fluid flows caused by torsional oscillations of the inner sphere in a thin spherical layer with respect to the state of rest. We show that an increase in the frequency of torsional oscillations leads to a change in the mode of the instability, with a transition from secondary flows in the form of Taylor vortices to the structures, which were not previously observed. The revealed instability is found in the frequency range from 0.61 to 2.45 Hz or, if the wavelengths are taken relative to the layer thickness, from 0.67 to 1.33.

1. Introduction

Flows caused by torsional oscillations can be used to determine rheological properties of fluids [1] and for intensifying filtration [2]. Periodic perturbations in the velocity may affect the transition to turbulence [3, 4]. Therefore it is important to have information on the stability limit and on the structure of secondary flows [1, 5].

A possible dependence of the secondary flow structures and the types of instability of the oscillation frequency is of special interest. Such dependence was revealed based on the measurements of velocity fields in a cylindrical thin layer $\beta = (r_2 - r_1)/r_1 = 0.087$, where r_1 and r_2 are the inner and outer radii [1, 5]. The structures resembling Taylor and Görtler vortices were observed in the low and high frequency limits, respectively. Subsequently, there was a knowledge gap about the structures in the intermediate frequency range. In a spherical layer with $\beta = 4.3$ [6] at torsional oscillations of the inner sphere the structure of secondary flows in two-dimensional calculations remains constant over a wide range of frequency variations. At other values of β, the dependence of the instability type on the frequency in spherical layers has not been previously studied.

The aim of this work is a numerical investigation of how the form of the secondary flow structures and stability limit depend on the frequency at torsional oscillations of the inner sphere with respect to the state of rest. To enable qualitative comparison of our results with [1, 5], we model a thin layer $\beta = 0.19$ in which Taylor vortices appear at a constant rotational speed of the inner sphere at the stability limit [7].

2. Methodology

An isothermal flow of a viscous incompressible fluid is described by the Navier–Stokes and continuity equations:

$$\frac{\partial \boldsymbol{U}}{\partial t} = \boldsymbol{U} \times \mathrm{rot}\boldsymbol{U} - \mathrm{grad}\left(\frac{p}{\rho} + \frac{\boldsymbol{U}^2}{2}\right) - \nu \mathrm{rotrot}\boldsymbol{U},\ \mathrm{div}\boldsymbol{U} = 0.$$

We use a spherical coordinate system with radial r, polar θ, and azimuthal φ directions. The no-slip and non percolation conditions at the boundaries have the form: $u_\varphi(r = r_{1,2}) = \Omega_{1,2}(t)r_{1,2}\sin\theta$, $u_r(r = r_{1,2}) = 0$, $u_\theta(r = r_{1,2}) = 0$, where 1 denotes conditions for the inner sphere and 2 – for the outer one. Here, U, p, and ρ are the velocity, pressure, and density of the fluid; u_φ, u_r, and u_θ are the azimuthal, radial, and polar components of the velocity, respectively. Ω_k is the angular rotational speed of the corresponding sphere and ν is the kinematic viscosity of the fluid in the layer. The rotational speed of the inner sphere varies periodically: $\Omega_1(t) = A\sin(2\pi ft)$, where A and f are the modulation amplitude and the frequency. The outer sphere is immobile: $\Omega_2 = 0$. We have used the algorithm and numerical solution program [8] based on a finite-difference spatial discretization scheme for the Navier–Stokes equations and a semi-implicit Runge–Kutta scheme for integration with respect to time. The spatial discretization was performed with decreasing cell size near the boundaries (with respect to r) and the equatorial plane (with respect to θ). The ratio of the maximum to minimum cell size varied from 2 to 5 with a total number of nodes up to $4.6\text{x}10^5$. The computations were performed at the following dimension parameters: $\nu = 5 \times 10^{-5}$ m^2/s, $r_1 = 0.126$ m, $r_2 = 0.15$ m, and $f = 0.0682$–4.363 Hz. In this case, thickness of the dynamic boundary layer is $\delta = (\nu/(\pi f))^{1/2} = (1.91-15.3)10^{-3}$m and minimum size δ corresponds to the seven nodes of the computational grid. The character of the flow depends on the quantities A, f, r_1,r_2 and ν and is determined by the three similarity parameters. These similarity parameters are relative layer thickness β, dimensionless wavelength $L = \lambda/(r_2 - r_1)$, where $\lambda = 2\pi\delta$, and the Reynolds number $\mathrm{Re} = (Ar_1^2/\nu)(\delta/r_1)$ [6].

3. Results and Discussion

Oscillations of the inner sphere cause circulation in the meridional plane of the flow [6, 9]. The circulation is similar to that at a constant rotational speed [7], but periodically varies with a double modulation frequency. The evolution of such flow in time before it loses its stability has already been well studied (see e.g. [6]). The flow structure was determined by the form of the azimuthal vorticity component [10] in the meridional plane ω_φ:

$$\omega_\varphi = \frac{1}{rr'}\frac{\partial r u_\theta}{\partial r} - \frac{1}{r\theta'}\frac{\partial u_r}{\partial \theta}$$

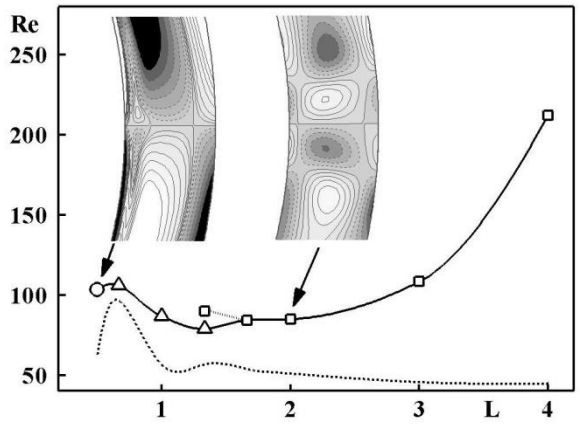

Figure 1. Stability limit (solid line) and difference of oscillation phases E_φ and E_ψ (dotted line). Shown here are levels ω_φ [s^{-1}] ($-10 < \omega_\varphi < 10$). On the right: Taylor vortices at L = 2, Re = 84.7, and $\Delta\omega_\varphi = 2$ (squares).On the left: Görtler vortices at L = 0.5, Re = 105.9, and $\Delta\omega_\varphi = 0.5$ (circle). The dotted lines for the levels ω_φ correspond to the counterclockwise direction. The triangles show the instability at intermediate wavelengths.

The attenuation decrement of the azimuthal velocity in the radial direction increases with increasing f until loss of stability [9]. This leads to a decrease in M_{out} (i.e., in the amplitude of the friction torque transferred to the outer sphere). Near the stability limit (both before and after it), the flow is symmetric with respect to the rotation axis and equatorial plane. All flow parameters vary with frequencies f or $2f$. Following [8], supercritical values of Re were used as initial conditions. The stability limit was determined by decreasing Re at f = const according to the form of the flow structure, magnitude of M_{out}, and ratio E_ψ/E_φ (where $E_\varphi = \int u_\varphi^2$ and $E_\psi = \int (u_r^2 + u_\theta^2)$ are the azimuthal and meridional components of the kinetic energy of the flow determined by integration over the whole volume of the spherical layer).

Our results demonstrate that, after the loss of stability, unsteady toroidal structures are formed in the flow near the equatorial plane. Their characteristic size decreases with a decrease in L and the meridional circulation (MC) is pushed back to the poles. In the case of long waves ($1.66 \le L \le 4$), the thoroughly studied Taylor vortices are formed at the stability limit. Their direction of rotation is opposite of the MC direction (Figure 1). The formation and decay of the vortices occur with hysteresis. At $L \le 2$, the vortices exist during the whole oscillation cycle. At L = 4, the vortices are observed during almost the whole cycle, with the exception of two small intervals when $\Omega_1(t)$ approaches A ($0.075 < tf < 0.177$ and $0.581 < tf < 0.676$, where t is the time from the beginning of the oscillation cycle, the left boundaries of the intervals correspond to the decay of vortices, and the right boundaries correspond to the beginning of the formation). At L = 3, the vortices observed in the region of the maximum of $\Omega_1(t)$ ($0.12 < tf < 0.3$ and $0.6 < tf < 0.8$). The Taylor vortices change their configuration during the oscillation period: during the formation, they are expanded in the radial direction; by the instant of decay, the dimensions in r and θ are close. The stability limit for Taylor vortices has a minimum at $1.66 \le L \le 2$ (Figure 1). Taylor vortices are also observed at L = 1.33. In this case, however, they are formed above the stability limit: the leftmost square in Figure 1 (Re = 91.1) and squares in Figure 2. At the same time, the flow is stable at Re ≤ 80.9.

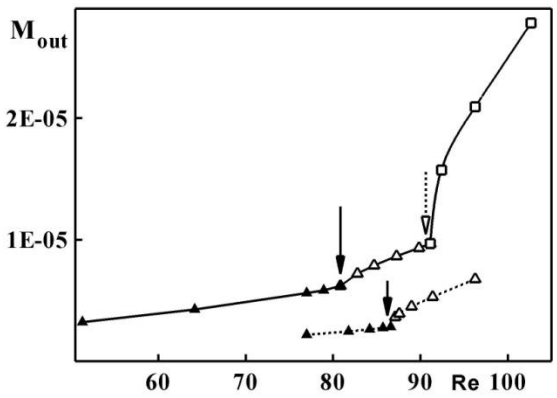

Figure 2. Quantity M_{out} normalized by the liquid density as a function of the Re number at L = 1.33 (solid line) and 1.0 (dotted line). The dark symbols correspond to the stable flow and the light ones - to the unstable flow. The first and second bifurcations are shown by the arrows with a solid and dotted lines, respectively.

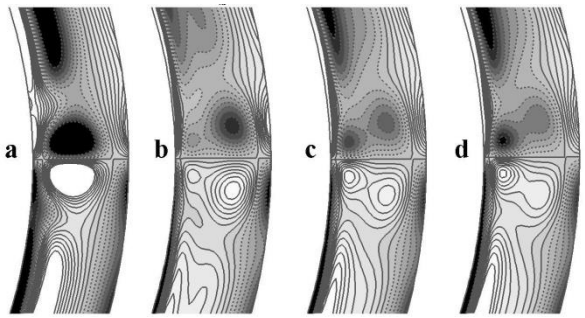

Figure 3. Distribution of the levels ω_φ [s^{-1}] in the meridional plane of the flow at L = 1.33 and Re = 80.8, $-8 < \omega_\varphi < 8$, and $\Delta\omega_\varphi = 1$. tf = (a) 0, 0.5; (b) 0.25, 0.75; (c) 0.28, 0.78; and (d) 0.3, 0.8. t is the time from the beginning of the oscillation cycle.

Thus, at L = 1.33, the transition to Taylor vortices is preceded by another type of instability. This type of instability is observed in the interval of intermediate wavelengths $0.67 \le L \le 1.33$ (triangles in Figures 1, 2).The structure of the secondary flow in this case is shown in Figure 3. The direction of the

vortex rotation near the equatorial plane coincides with the MC direction and the characteristic scale does not exceed half of the layer thickness. Let us consider the evolution of these structures in time. With an increase in $\Omega_1(t)$ from 0 (Figure 3a) to *A* (Figure 3b), individual vortices are pushed back from the inner sphere and from the equatorial plane. Two vortices are formed. The vortex with the maximum ω_φ is closer to the outer boundary. Later, with a decrease in $\Omega_1(t)$ (Figure 3c), a rapid redistribution of ω_φ occurs: the maximum is shifted to the inner sphere, then this maximum enhances (Figure 3d), and the flow returns to the initial state (Figure 3a). The minimum of the stability limit is observed near L = 1.33. At L < 1.33, an increase in Re is accompanied not by the transition to Taylor vortices but by the transition to a flow without the axial and equatorial symmetries. At the same time, the direction of vortex rotation in the secondary flow remains the same.

In the case of short waves (L = 0.5), at the stability limit after passing the extreme values ($0.28 < tf < 0.31$ and $0.78 < tf < 0.81$), vortices with a characteristic scale that is much less than the layer thickness are formed near the inner sphere and equatorial plane (Figure 1). The typical size, rotation direction (opposite to the MC direction), and sharp change in the quantity ω_φ near the inner sphere may imply that Görtler vortices caused by the instability of the dynamic boundary layer are observed in this case. Probably, at L = 0.67, the instability in the form of Görtler vortices precedes the instability at intermediate wavelengths (Figure 3), just as the instability at intermediate wavelengths precedes Taylor vortices at L = 1.33 (Figure 1).

4. Summary

At torsional oscillations of the inner sphere in a thin layer $\beta = 0.19$, three types of instability are observed, and each type is associated with its own variation range of dimensionless wavelength L. The boundaries of the ranges can be determined by the position of maxima of both, the stability limit and the phase difference between E_φ and E_ψ depending on L (Figure 1). The toroidal structures forming at the stability limit near the equatorial plane in the case of short ($L \leq 0.5$) and long ($L \geq 1.67$) waves qualitatively correspond to the results of experiments [1, 5]. The rotation direction for them is opposite to the MC direction. At the instability revealed at intermediate wavelengths ($0.67 \leq L \leq 1.33$ and $2.45 \geq f \geq 0.61$ Hz), rotation directions of the vortices and MC coincide. The results of our calculations imply that further experimental verification of the revealed instability relies on measuring not only velocity fields (as it was done, e.g., in [1, 5]), but also friction torques.

Acknowledgments

This work was supported by the Russian Foundation for Basic Research project No. 16-05-00004 and 18-08-00074. MG acknowledges, in part, support from the ERC Advanced Grant No. 320773. Research at the Ural Federal University is supported by the Act 211 of the Government of the Russian Federation, agreement No 02.A03.21.0006. We thank Dr. Laura K. Zschaechner (University of Helsinki, Finnish Center for Astronomy with ESO) for her help with language corrections.

References

[1] Fardin M, Perge C, Casanellas L, Hollis T, Taberlet N, Ortin J, Lerouge S and Manneville S 2014 *Rheol. Acta* **53** 885
[2] Jaffrin M 2012 *Ann. Rev. Fluid Mech*. **44** 77
[3] Zhilenko D Yu and Krivonosova O E 2015 *Tech. Phys. Lett*. **41** 5
[4] Bountin D A and Maslov A A 2017 *Tech. Phys. Lett*. **43** 623
[5] Fardin M, Perge C, Taberlet N and Manneville S 2014 *Phys. Rev.E* **89** 011001
[6] Hollerbach R, Wiener R, Sullivan I, Donnelly R, and Barenghi C 2002 *Phys. Fluids* **14** 4192
[7] Belyaev Yu N and Yavorskaya I M 1980 *Itogi Nauki Tekh. Ser. Mekh. Zhidk. Gaza* **15** 3
[8] Nikitin N 2006 *J. Comp. Phys*. **217** 759
[9] Zhilenko D Yu and Krivonosova O E 2016 *JETP Lett*. **104** 527
[10] Landau L D and Lifshitz E M 1986 *Course of Theoretical Physics*, *Vol. 6: Fluid Mechanics* Pergamon, New York.